Stilbene Glucoside from *Polygonum multiflorum* Thunb.: A Novel Natural Inhibitor of Advanced Glycation End Product Formation by Trapping of Methylglyoxal

LISHUANG LV,[†,‡,§] XI SHAO,[‡,§,#] LIYAN WANG,[‡] DERONG HUANG,[‡,§] CHI-TANG HO,[#] AND SHENGMIN SANG*[,‡,§]

[†]Department of Food Science and Technology, Ginling College, Nanjing Normal University, 122 Ninghai Road, Nanjing 210097, People's Republic of China, [‡]Human Nutrition Research Program, Julius L. Chambers Biomedical/Biotechnology Research Institute, North Carolina Central University, North Carolina Research Campus, 500 Laureate Way, Kannapolis, North Carolina 28081, [§]Center of Excellence for Post-harvest Technologies, North Carolina Agricultural and Technical State University, North Carolina Research Campus, 500 Laureate Way, Suite 4222, Kannapolis, North Carolina 28081, and [#]Department of Food Science, Rutgers University, 65 Dudley Road, New Brunswick, New Jersey 08901-8520

Methylglyoxal (MGO), the reactive dicarbonyl intermediate generated during the nonenzymatic glycation between reducing sugars and amino groups of proteins, lipids, and DNA, is the precursor of advanced glycation end products (AGEs). Many studies have shown that AGEs play a major pathogenic role in diabetes and its complications. This study found that 2,3,5,4′-tetrahydroxystilbene 2-O-β-D-glucoside (THSG), the major bioactive compound from *Polygonum multiflorum* Thunb., can efficiently inhibit the formation of AGEs in a dose-dependent manner by trapping reactive MGO under physiological conditions (pH 7.4, 37 °C). More than 60% MGO was trapped by THSG within 24 h, which was much more effective than resveratrol and its methylated derivative, pterostilbene, the two major bioactive dietary stilbenes. The major mono- and di-MGO adducts of THSG were successfully purified and found to be mixtures of tautomers. LC-MS and NMR data showed that positions 4 and 6 of the A ring were the major active sites for trapping MGO. It was also found that THSG could significantly inhibit the formation of AGEs in the human serum albumin (HSA)−MGO assay and both mono- and di-MGO adducts of THSG were detected in this assay using LC-MS. The results suggest that the ability of THSG to trap reactive dicarbonyl species makes it a potential natural inhibitor of AGEs.

KEYWORDS: 2,3,5,4′-Tetrahydroxystilbene 2-O-β-D-glucoside (THSG); stilbene glucoside; *Polygonum multiflorum* Thunb.; methylglyoxal; advanced glycation end products (AGEs)

INTRODUCTION

Diabetes is the fifth most deadly disease in the United States. Most diabetes patients die from diabetic complications, such as renal failure, heart attack, or stroke. However, diabetic complications are still neither preventable nor curable. New agents that can prevent, treat, and cure diabetic complications are needed. Increasing evidence has identified the formation of advanced glycation end products (AGEs) as a major pathogenic link between hyperglycemia and diabetes-related complications (1). α-Oxoaldehydes such as methylglyoxal (MGO), the reactive dicarbonyl intermediate generated during the nonenzymatic glycation between reducing sugars and amino groups of proteins, lipids, and DNA, are precursors of AGEs and exert direct toxicity to cells and tissues (2−4). Trapping of reactive dicarbonyl compounds by several pharmaceutical agents, such as aminoguanidine, metformin, and pyridoxamine, has been shown to be a useful strategy for inhibiting the formation of AGEs and, thus, inhibiting or delaying diabetic complications (5−10).

In our studies to find nontoxic trapping agents for reactive dicarbonyl species from dietary sources, we found that flavonoids, such as (−)-epigallocatechin 3-gallate (EGCG) from tea, and phloretin and phloridzin from apple, can efficiently trap reactive dicarbonyl compounds (MGO or GO) to form mono- and di-MGO or GO adducts (11, 12). To investigate whether this finding applies to other types of compounds and to gain more understanding of the structure−activity relationship, we further studied the trapping efficacy of dietary stilbene using 2,3,5,4′-tetrahydroxystilbene 2-O-β-D-glucoside (THSG) (**Figure 1**) as the representative compound.

THSG (**Figure 1**) is the major bioactive component from *Polygonum multiflorum* Thunb., which is also known as He-Shou-Wu in China and Fo-ti in North America. *P. multiflorum* has been used in China and Japan as a tonic and antiaging agent

*Corresponding author [telephone (704) 250-5700; fax (704) 250-5709; e-mail ssang@ncat.edu].
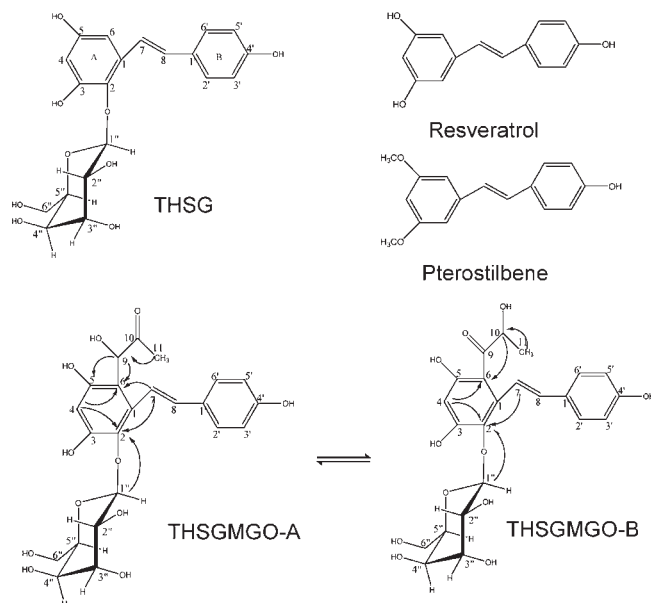
Figure 1. Chemical structures of 2,3,5,4′-tetrahydroxystilbene 2-*O*-β-D-glucoside (THSG), resveratrol, pterostilbene, and the mono-MGO conjugated THSG adducts THSGMGO-A and THSGMGO-B and significant HMBC (H→C) correlations of THSGMGO-A and THSGMGO-B.

since ancient times (*13*). It is a close relative of *Polygonum cuspidatum*, from which resveratrol was originally purified (*14*). Similar to resveratrol, THSG has been reported as a strong natural antioxidative and anti-inflammatory agent (*15−18*). In this study, we investigated whether THSG could inhibit the formation of AGEs by trapping reactive dicarbonyl compounds, such as MGO, under physiological conditions.

MATERIALS AND METHODS

Materials. THSG was purified from *P. multiflorum* Thunb in our laboratory. Pterostilbene was provided by Sarbinsa Corp. (Piscataway, NJ). Resveratrol, methylglyoxal (MGO, 40% in water), 1,2-diaminobenzene (DB), CD$_3$OD, Sephadex LH-20 gel, and analytical (250 μm thickness, 2−25 μm particle size) and preparative TLC plates (2000 μm thickness, 2−25 μm particle size) were purchased from Sigma (St. Louis, MO). HPLC-grade solvents and other reagents were obtained from VWR Scientific (South Plainfield, NJ). HPLC-grade water was prepared using a Millipore Milli-Q purification system (Bedford, MA).

Kinetic Study of the Trapping of MGO by THSG, Pterostilbene, and Resveratrol under Physiological Conditions. MGO (0.33 mM) with 1 mM THSG, pterostilbene, and resveratrol, respectively, in a pH 7.4 phosphate buffer solution (100 mM) was shaken at 40 rpm and incubated at 37 °C for 0, 10, 30, 60, 120, 240, 420, or 1440 min. Then, to each triplicated vial at each time point was added 1 μL of acetic acid to stop the reaction, and 100 mM DB was added next to derivatize the remaining MGO using our previous method (*12*).

UPLC Analysis. The level of methylquinoxaline was analyzed by a Waters Acquity UPLC system coupled with a PDA detector (Waters, Milford, MA). We used a 50 mm × 2.1 mm inner diameter, 1.7 μm, Waters BEH RP-C18 column. For binary gradient elution, mobile phases A (90% water, 10% methanol, and 0.2% acetic acid) and B (100% methanol with 0.2% acetic acid) were used. The flow rate was maintained at 0.5 mL/min, and the mobile phase began with 100% A. It was followed by progressive linear increases in B to 20% at 1.5 min, to 35% at 2.5 min, and to 100% at 4.5 min. Then, the mobile phase was maintained at 100% B until 5.5 min and re-equilibrated to 100% A from 5.6 to 7.0 min. The injection volume was 5 μL for each sample. The level of methylquinoxaline was quantified at 313 nm.

LC-MS Analysis. A Thermo LC/ESI-MS system equipped with a Surveyor MS pump, a Surveyor refrigerated autosampler, and an LCQ linear ion trap mass detector (Thermo Finnigan, San Jose, CA) incorporated

Table 1. δ_H (700 MHz) and δ_C (175 MHz) NMR Spectral Data of THSGMGO-A and THSGMGO-B (CD$_3$OD) (δ in Parts per Million and *J* in Hertz)

| | THSG | | THSGMGO | | | |
| | | | δ_H | | δ_C | |
	δ_H	δ_C	A (or B)	B (or A)	A (or B)	B (or A)
1		129.96 s			131.11 s	131.17 s
2		137.81 s			139.11 s	138.70 s
3		152.06 s			153.26 s	153.19 s
4	5.93 br s	102.42 d	6.02 s	5.95 s	98.37 d	98.46 d
5		155.90 s			158.51 s	158.51 s
6	6.31 br s	108.20 d			116.81 s	116.81 s
7	7.42 d, *J*16.4	121.42 d	7.52 d, *J*16.0	7.48 d, *J*16.0	116.61 d	116.61 d
8	6.6 d, *J*16.4	133.51 d	7.20 d, *J*16.0	7.18 d, *J*16.0	134.72 d	134.31 d
1′		130.69 s			132.22 s	132.25 s
2′	7.14 d, *J*7.8	129.23 d	7.25 d, *J*7.7	7.25 d, *J*7.7	129.37 d	129.41 d
3′	6.45 d, *J*7.4	116.34 d	6.51 d, *J*7.9	6.51 d, *J*7.9	116.33 d	116.34 d
4′		158.29 s			158.39 s	158.34 t
5′	6.45 d, *J*7.4	116.34 d	6.51 d, *J*7.9	6.51 d, *J*7.9	116.33 d	116.34 d
6′	7.14 d, *J*7.8	129.23 d	7.25 d, *J*7.7	7.25 d, *J*7.7	129.37 d	129.41 d
1″	4.19 d, *J*7.8	103.42 d	4.32 d, *J*7.4	4.25 d, *J*7.5	107.88 d	108.29 d
2″	3.49 m	75.36 d	3.34 m	3.34 m	75.30 d	75.30 d
3″	3.25 m	78.07 d	3.18 m	3.18 m	78.42 d	78.40 d
4″	3.26 m	70.38 d	3.29 m	3.29 m	70.43 d	70.43 d
5″	2.95 m	77.77 d	2.95 m	2.95 m	77.79 d	77.72 d
6″	3.48 m	61.78 t	3.46 m	3.46 m	61.74 t	61.77 t
	3.49 m		3.53 m	3.53 m		
9			4.58 m		78.16 d	nd[a]
10				3.68 m	nd	64.73 d
11			1.40 s	0.90 d 3.4	21.71 q	25.23 q

[a] nd, not detected.

with an electrospray ionization (ESI) interface was used. A Gemini C18 column (50 mm × 2.0 mm i.d., 3 μm, Phenomenex) was used for the analysis of the reaction products with a flow rate of 0.2 mL/min. The binary mobile phase system consisted of 10% aqueous methanol with 0.2% acetic acid as A and 90% aqueous methanol with 0.2% acetic acid as B. The column was eluted with isocratic phase A for 5 min followed by a gradient progress (from 100 to 90% A from 5 to 10 min; from 90 to 60% A from 10 to 36 min; from 60 to 0% A from 36 to 40 min, then 100% A from 41 to 51 min). The injection volume was 10 μL for each sample. The column temperature was maintained at 20 °C. The negative ion polarity mode was set for the ESI ion source with the voltage on the ESI interface maintained at approximately 5 kV. Nitrogen gas was used as both the sheath gas at a flow rate of 30 arb units and the auxiliary gas at 5 arb units. The structural information of THSG and the major MGO adducts was obtained by tandem mass spectrometry (MS/MS) through collision-induced dissociation (CID) with a relative collision energy setting of 35%.

Determining the Formation of MGO Adducts of THSG Using LC-MS. THSG (1.0 mM) was incubated with different concentrations of MGO (0.33, 1.0, and 3.0 mM) in a pH 7.4 phosphate buffer solution at 37 °C for 8 h. Then, 10 μL samples were taken and transferred to vials containing 190 μL of a solution consisting of 0.2% acetic acid to stabilize THSG and related MGO adducts. These samples were either immediately analyzed by LC-MS or stored at −80 °C.

NMR Analysis. ^{1}H (700 MHz), ^{13}C (175 MHz), and all 2D NMR spectra were acquired on a Bruker 700 MHz instrument. All compounds were analyzed in CD$_3$OD, with TMS as the internal standard. ^{1}H−^{13}C HMQC (heteronuclear multiple quantum correlation) and HMBC (heteronuclear multiple bond correlation) experiments were performed as described previously (*19*).

Purification of the Major MGO Adducts of THSG. THSG (0.102 g, 50 mM) and MGO (0.135 g, 150 mM) were dissolved in 5 mL of phosphate buffer (100 mM, pH 7.4) and then kept at 37 °C for 24 h. The reaction mixture was loaded onto a Sephadex LH-20 column eluted with ethanol to obtain mono-MGO conjugated THSG (73 mg) and a mixture of THSG and mono- and di-MGO conjugated THSG. This mixture was then applied to preparative TLC plates and developed with ethyl acetate/methanol/water (20:2:1, v/v) to obtain 13 mg di-MGO conjugated THSG.

^{1}H and ^{13}C NMR data of THSG and mono-MGO conjugated THSG are listed in **Table 1**.

Effect of THSG on the Formation of AGEs in the HSA−MGO Assay. HSA (1.4 mg/mL) was incubated with methylglyoxal (500 μM) in the presence (0.25, 0.5, 1.0, 2.0 mM) or absence of THSG in phosphate buffer (pH 7.4) at 37 °C. A mixed streptomycin (0.5 mg)/penicillin (500 units) solution was added into the reaction solutions to prevent
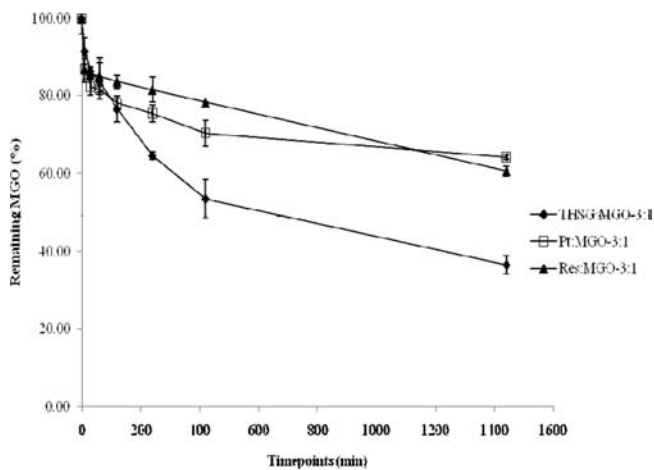

Figure 2. Trapping of MGO by THSG, resveratrol (Res), and pterostilbene (Pt) under physiological conditions (pH 7.4, 37 °C).

bacterial growth. Then, 500 μL of sample was collected at different time points (0, 1, 2, 4, 7, and 30 days) and stored at −80 °C. A multimode microplate reader (BioTek, Winooski, VT) was used for the quantification of AGEs. The fluorescence of samples was measured at an excitation/emission wavelength of 370/440 nm. Percent inhibition of formation of AGEs by each sample was calculated using the following equation: % inhibition = [1 − (fluorescence of the solution with inhibitors/fluorescence of the solution without inhibitors)] × 100%.

Determining the Formation of MGO Adducts of THSG in the HSA−MGO System Using LC-MS. Samples collected at day 4 from the THSG (250 μM, 500 μM, 1.0 mM, and 2.0 mM) treated HSA−MGO system, and the purified mono- and di-MGO conjugated THSG were analyzed using the LC-MS method described above.

RESULTS AND DISCUSSION

Trapping of MGO by THSG, Pterostilbene, and Resveratrol under Physiological Conditions. Our results indicated that THSG, pterostilbene, and resveratrol can effectively trap MGO under physiological conditions (**Figure 2**). Among them, THSG was the most effective trapping agent. More than 60% of MGO was trapped within 24 h by THSG, and <40% of MGO was trapped by resveratrol and pterostilbene (**Figure 2**). In addition, we found that none of the three compounds could trap MGO under acidic conditions (pH 4).

Studying the Formation of MGO Adducts of THSG by LC-MS. The reaction mixtures of THSG with MGO under three different ratios (3:1, 1:1, and 1:3) were analyzed by LC-MS. After 8 h of
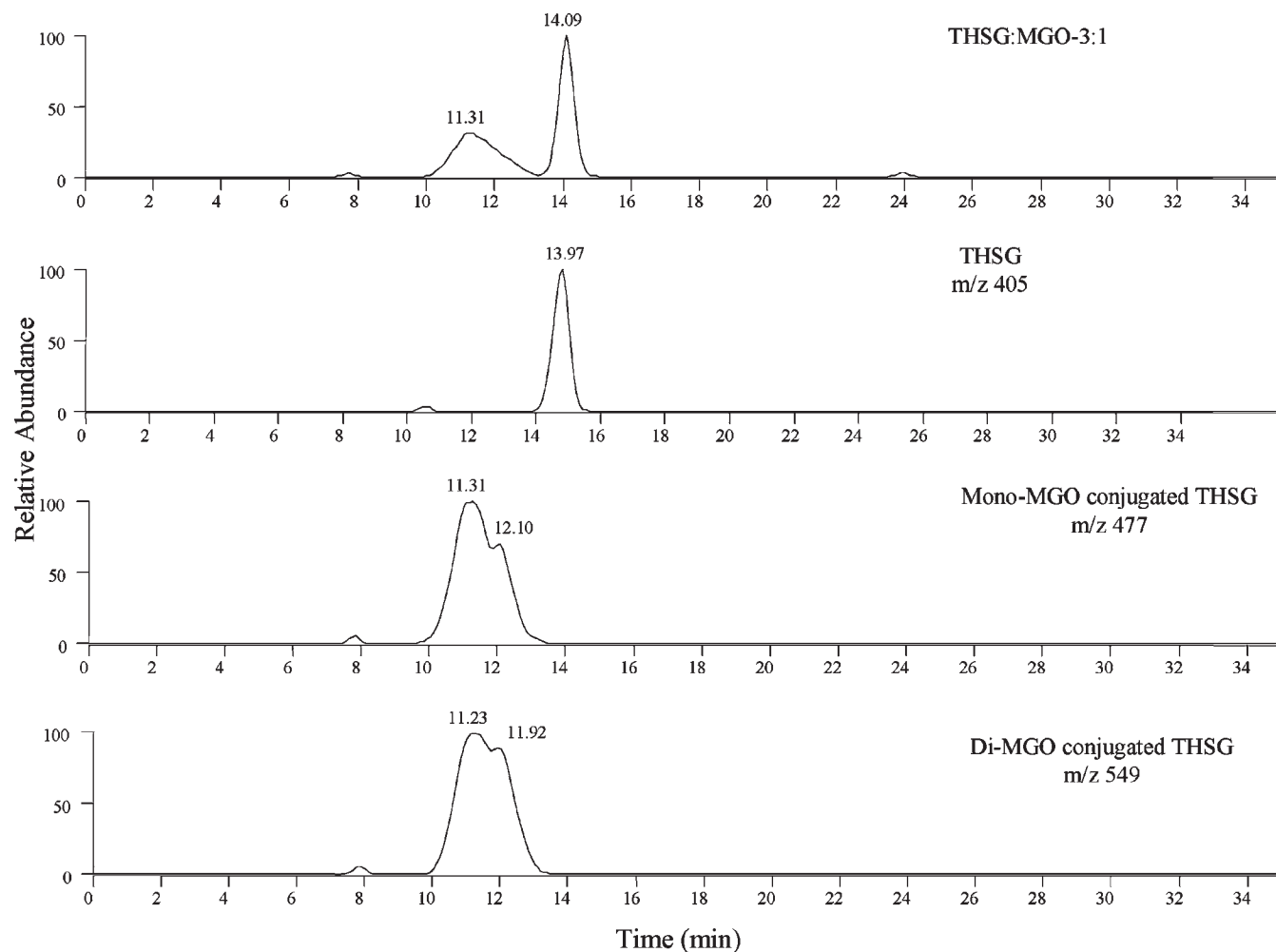

Figure 3. LC chromatogram of THSG after incubation with MGO (3:1) for 8 h. The chromatograms of THSG and mono- and di-MGO adducts of THSG were obtained using the selective ion monitoring mode.
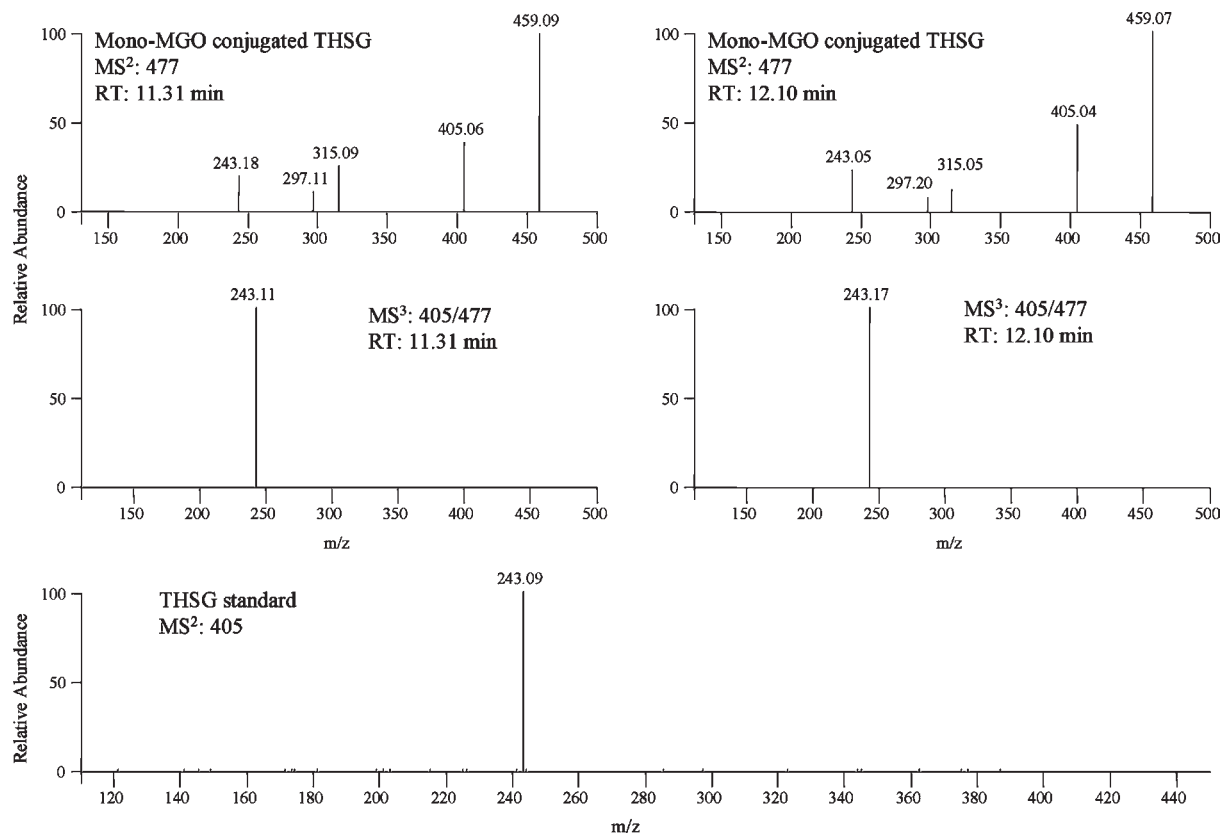
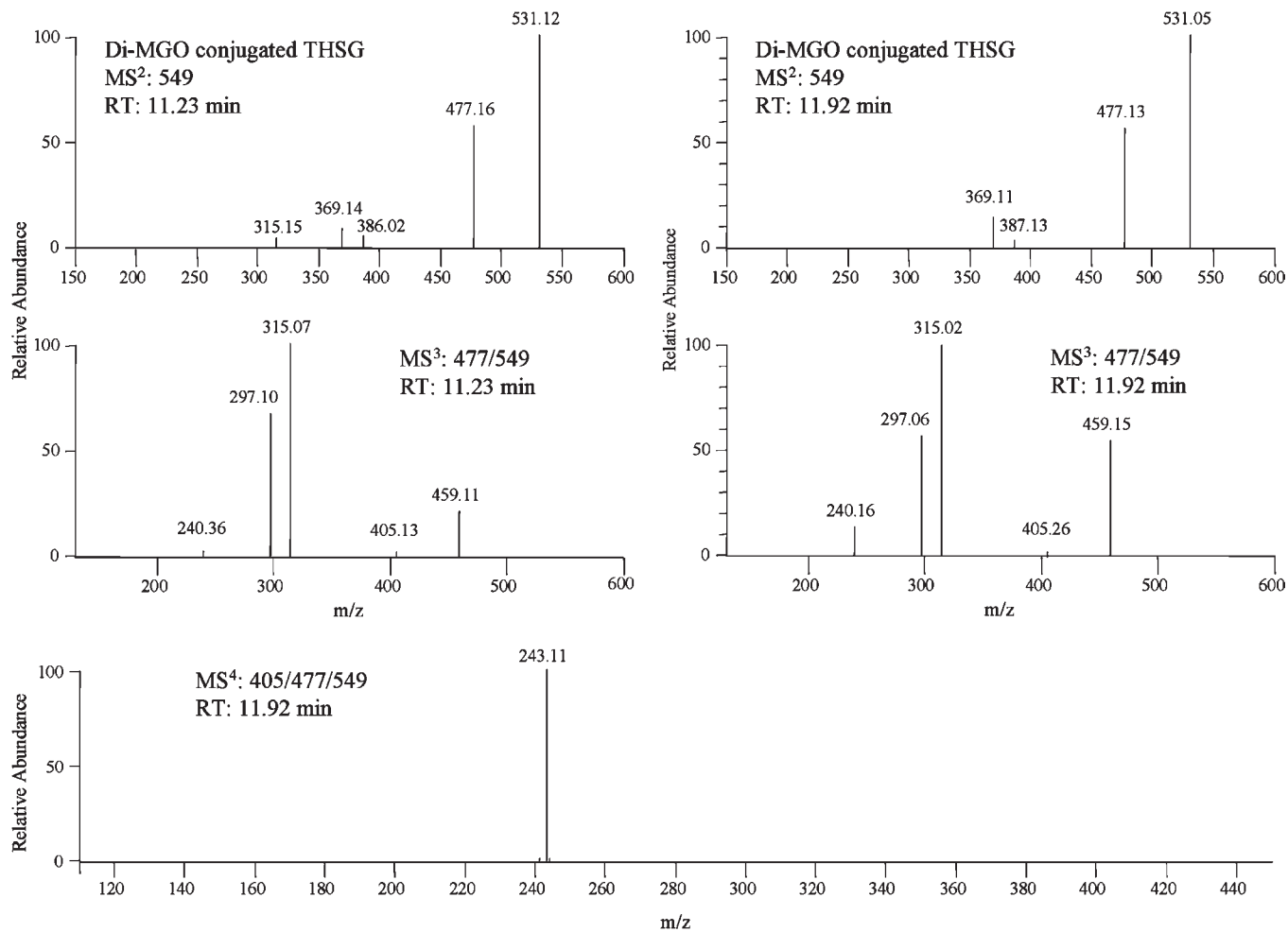**Figure 4.** Tandem MS/MS spectral of mono-MGO adducts of THSG and THSG standard.

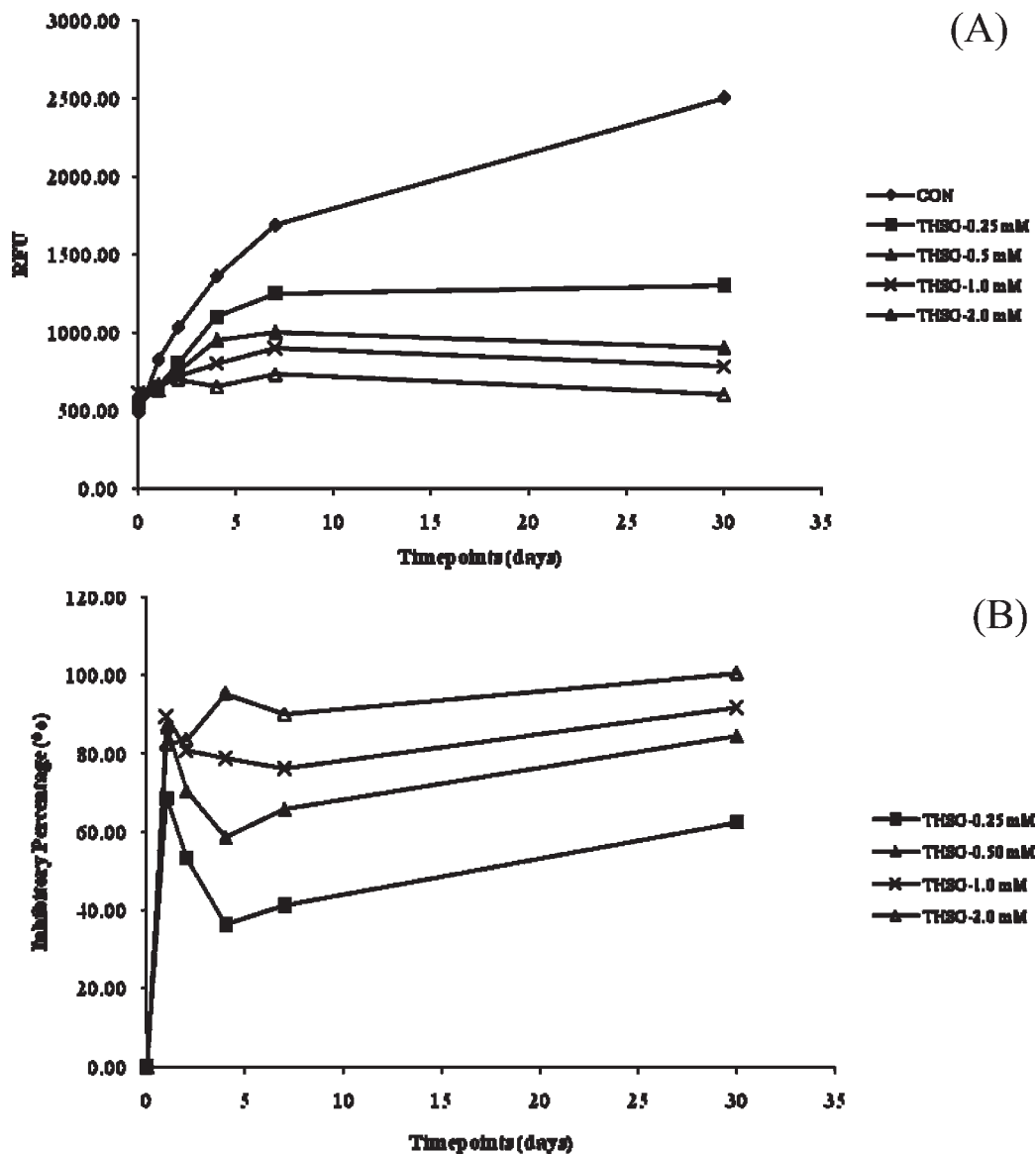**Figure 5.** Tandem MS/MS spectral of di-MGO adducts of THSG.

Figure 6. Dose-dependent inhibitory effect of the formation of AGEs by THSG: (**A**) formation of AGEs; (**B**) percent inhibition of the formation of AGEs.

incubation of THSG with MGO (3:1 ratio), one broad peak appeared in the LC chromatogram (RT 11.31 min), which was a mixture of mono- and di-MGO adducts of THSG (**Figure 3**). This broad peak had the molecular ions m/z 477 ([M − H]⁻; mono-MGO adducts) and m/z 549 ([M − H]⁻; di-MGO adducts). Under selective ion monitoring (SIM) mode for m/z 477 ([M − H]⁻; mono-MGO adducts), two broad peaks appeared in the LC chromatogram (**Figure 3**). Both peaks had the same molecular ion (m/z 477 [M − H]⁻) and MS/MS fragments, but different retention times. Both peaks had the fragment ion m/z 405 ([M − 72 − H]⁻), showing that they all lost one MGO (m/z 72) molecule (**Figure 4**), thus indicating that they were mono-MGO adducts of THSG. In addition, the MS/MS spectrum of this daughter ion (MS³ 405/477) was identical to the MS/MS spectrum of the standard THSG (MS² 405) (**Figure 4**). All of these features indicated that both peaks were the mono-MGO conjugated THSG.

Under SIM mode for m/z 549 ([M − H]⁻; di-MGO adducts), two broad peaks appeared in the LC chromatogram, which had retention times very similar to those for the mono-MGO adducts (**Figure 3**). We tried several different reverse phase HPLC columns, but failed to separate mono- and di-MGO conjugated THSG. The two peaks had the same molecular ion (m/z 549 [M − H]⁻) and

MS/MS fragments. Both of them had the fragment ion m/z 477 ([M − 72 − H]⁻) (**Figure 5**). The MS/MS spectrum of this daughter ion (MS³ 477/459) was similar to the MS/MS spectrum of the mono-MGO conjugated THSG (MS² 477) (**Figures 4** and **5**). It had the fragment ion m/z 405 ([M − 72 − 72 − H]⁻). The MS/MS spectrum of this daughter ion (MS⁴ 405/477/459) was identical to the MS/MS spectrum of the THSG standard (MS² 405) (**Figures 4** and **5**). This indicates that both peaks were di-MGO conjugated THSG.

Using THSG and MGO at a 1:1 ratio or 1:3 ratio, we found that the amounts of di-MGO adducts formed were higher than those from the reaction at a 3:1 ratio and the amount of THSG significantly decreased (data not shown).

Purification and Structure Elucidation of the Major MGO Adducts of THSG. To further confirm the structures of the major MGO adducts of THSG, we purified the major products from the reaction between THSG and MGO in 1:3 ratios using a Sephadex LH-20 column eluted with ethanol in combination with preparative normal phase silica gel TLC plates. Although the RP-C18 column could not separate mono-MGO and di-MGO adducts of THSG, we found that normal phase silica gel could separate them very well. Two major products were purified. Further LC-MS analysis of those two products indicated that one was the mixture
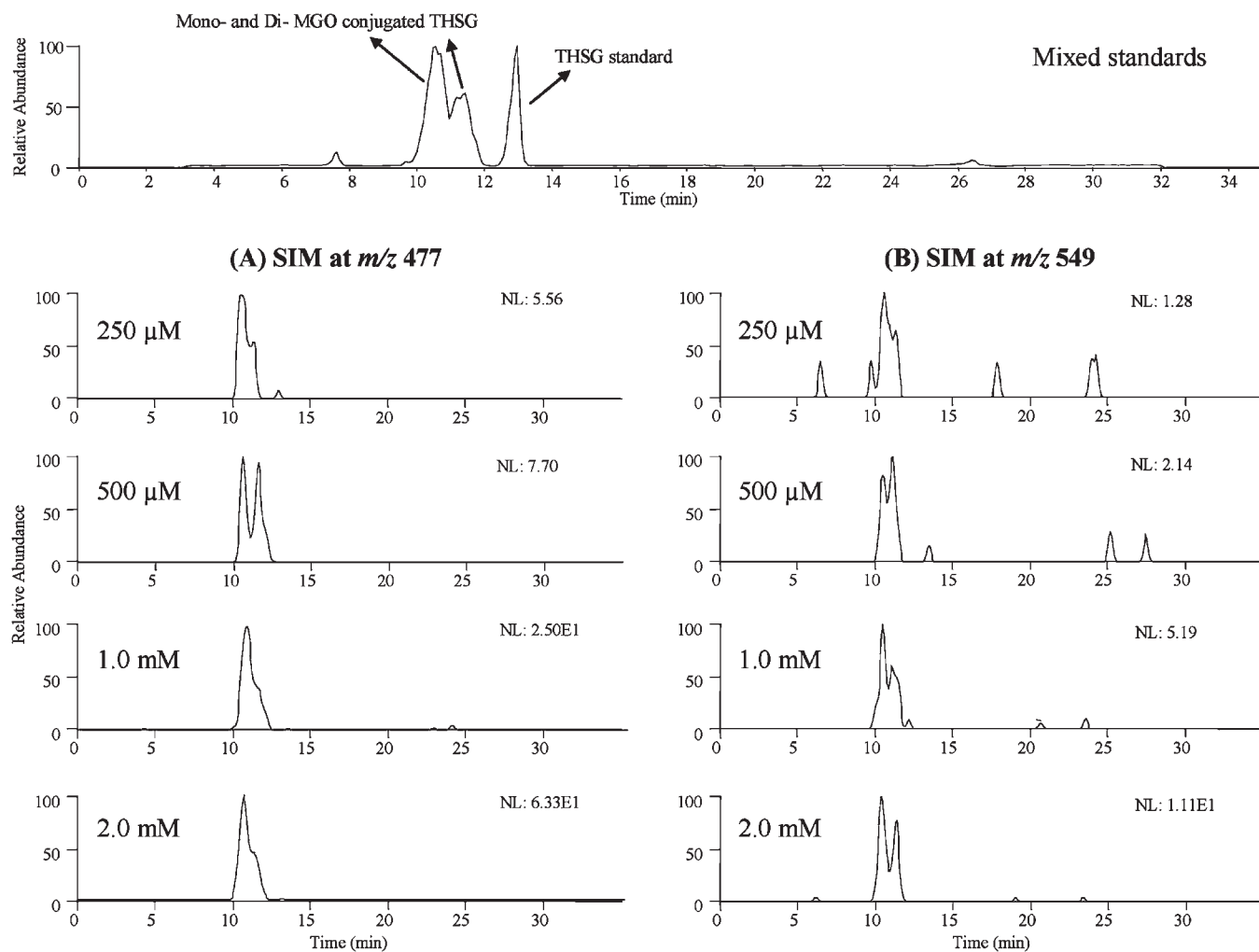
Figure 7. LC chromatogram of the mixture of THSG and mono- and di-MGO adducts of THSG. The chromatograms of mono- (**A**) and di-MGO (**B**) adducts of THSG were obtained using the selective ion monitoring (SIM) mode after incubation with THSG (250 μM, 500 μM, 1.0 mM, and 2.0 mM) in the HSA−MGO assay for 4 days.

of the mono-MGO adducts and the other one was the mixture of the di-MGO adducts.

The mono-MGO adducts (THSGMGO) had the molecular formula $C_{23}H_{26}O_{11}$ based on negative-ion ESI-MS (at m/z 477) and ^{13}C data. The molecular weight of THSGMGO was 72 (MW of MGO, 72) mass units higher than that of THSG. The ^1H and ^{13}C NMR spectra of THSGMGO showed two sets of mono-MGO conjugated THSG, which was consistent with the observation of two peaks in the LC chromatogram. All of these features indicate that this compound is a mixture of two tautomers (**Figure 1**). Both the ^1H and ^{13}C NMR spectra of THSGMGO had patterns very similar to those in the spectra of THSG (**Table 1**). The ^1H NMR spectrum of THSGMGO showed two distinct sets of aromatic ring proton signals: an AA′BB′ system with four protons, two at δ 6.51 and two at δ 7.25, indicating a para-substituted benzene ring, which was similar to those of THSG; and one singlet signal for one proton (δ 6.02 or 5.95 s), instead of the two broad singlets (2H) at δ 5.93 and δ 6.31 in the ^1H NMR spectrum of THSG, suggesting MGO conjugated with THSG at position 4 or 6 of the A ring. In comparison with the ^{13}C spectrum of THSG, THSGMGO had a quaternary carbon at δ_C 116.81 in its ^{13}C spectrum in lieu of an unsubstituted aromatic carbon from the A ring of THSG. All of these spectral features supported the presence of an MGO group in THSGMGO at either the C-4 or

C-6 position of the A ring. The HMBC spectrum showed a correlation between δ_C 139.11 (or 138.70) and H-1″ (δ_H 4.32 d, J = 7.4 Hz or 4.25 d, J = 7.4 Hz) of the glucose group, indicating δ_C 139.11 (or 138.70) was C-2 of the A ring. In addition, the only proton on the A ring (δ_H 6.02 or 5.95 s) showed a correlation to δ_C 139.11 (or 138.70), suggesting that this proton was H-4 and the MGO group was located at the C-6 position of the A ring. Thus, the structure of THSGMGO was identified as shown in **Figure 1**.

Even though we observed only one band for the second product that we purified using preparative normal phase silica gel TLC plates, its ^1H NMR and ^{13}C NMR spectra indicated that it was a mixture of several compounds. LC-MS analysis indicated that it was the mixture of di-MGO conjugated THSG.

Effect of THSG on the Formation of AGEs. Our results indicated that THSG could inhibit the formation of AGEs in a dose-dependent manner (**Figure 6**). At a 2 mM concentration, it could inhibit the formation of AGEs by >90% after 4 days of incubation, and >60% inhibition was observed after 30 days of incubation at 0.25 mM concentration (**Figure 6**).

Determining the Formation of MGO Adducts of THSG in the HSA−MGO System Using LC-MS. To further understand whether the inhibition of the formation of AGEs was due to the trapping of MGO by THSG, we determined the existence of the mono- and di-MGO conjugated THSG in the samples

collected after incubation of THSG with HSA and MGO using LC-MS. We found that both mono- and di-MGO conjugated THSG could be detected, and they had retention times and MS/MS spectra identical with those of the mono- and di-MGO adducts that we purified from the reaction between THSG and MGO (data not shown). In addition, their levels increased as the concentrations of THSG increased (**Figure 7**).

Our previous results indicated that both flavanol- and chalcone-type compounds could rapidly trap MGO under physiological conditions (*11*, *12*). In this study, we found that stilbene type compounds could also trap MGO under neutral or alkaline conditions. THSG, the major bioactive stilbene glucoside from a traditional Chinese herbal tea, *P. multiflorum* Thunb., had much stronger trapping effects than resveratrol and its methylated derivative, pterostilbene. The additional hydroxyl group in THSG could be the major factor that enhanced the trapping efficacy of THSG. We also found that THSG could inhibit the formation of AGEs in a dose-dependent manner.

To understand the mechanism by which THSG could trap reactive dicarbonyl species, we further studied the formation of MGO adducts of THSG using LC-MS and NMR. Therefore, our results clearly indicated that the two unsubstituted carbons at positions 4 and 6 on the A-ring were the major active sites for stilbene-type compounds to trap reactive dicarbonyl species. This was consistent with our previous finding that the two unsubstituted carbons at the A ring of EGCG (positions 6 and 8 for flavanol-type compounds) and phloretin (positions 3 and 5 for chalcone-type compounds) were the major active sites to trap reactive dicarbonyl species and form mono- and di-MGO adducts.

The formation of MGO adducts of THSG in the HSA−MGO system was determined by LC-MS analysis using the adducts purified from the reaction between THSG and MGO. Our results demonstrate for the first time that THSG could inhibit the formation of AGEs by trapping reactive dicarbonyl species. It is worthwhile to further study whether THSG can decrease the levels of reactive dicarbonyl compounds, such as MGO, and therefore inhibit the formation of AGEs and delay the development of diabetic complications under in vivo conditions.

LITERATURE CITED

(1) Singh, R.; Barden, A.; Mori, T.; Beilin, L. Advanced glycation endproducts: a review. *Diabetologia* **2001**, *44*, 129–146.

(2) Yim, H. S.; Kang, S. O.; Hah, Y. C.; Chock, P. B.; Yim, M. B. Free radicals generated during the glycation reaction of amino acids by methylglyoxal. A model study of protein-cross-linked free radicals. *J. Biol. Chem.* **1995**, *270*, 28228–28233.

(3) Kalapos, M. P. Methylglyoxal in living organisms: chemistry, biochemistry, toxicology and biological implications. *Toxicol. Lett.* **1999**, *110*, 145–175.

(4) Gugliucci, A. Glycation as the glucose link to diabetic complications. *J. Am. Osteopath. Assoc.* **2000**, *100*, 621–634.

(5) Thornalley, P. J. Use of aminoguanidine (Pimagedine) to prevent the formation of advanced glycation endproducts. *Arch. Biochem. Biophys.* **2003**, *419*, 31–40.

(6) Rahbar, S.; Figarola, J. L. Novel inhibitors of advanced glycation endproducts. *Arch. Biochem. Biophys.* **2003**, *419*, 63–79.

(7) Ruggiero-Lopez, D.; Lecomte, M.; Moinet, G.; Patereau, G.; Lagarde, M.; Wiernsperger, N. Reaction of metformin with dicarbonyl compounds. Possible implication in the inhibition of advanced glycation end product formation. *Biochem. Pharmacol.* **1999**, *58*, 1765–1773.

(8) Voziyan, P. A.; Metz, T. O.; Baynes, J. W.; Hudson, B. G. A post-Amadori inhibitor pyridoxamine also inhibits chemical modification of proteins by scavenging carbonyl intermediates of carbohydrate and lipid degradation. *J. Biol. Chem.* **2002**, *277*, 3397–3403.

(9) Beisswenger, P.; Ruggiero-Lopez, D. Metformin inhibition of glycation processes. *Diabetes Metab.* **2003**, *29* (4 Part 2), 6S95–S103.

(10) Nagaraj, R. H.; Sarkar, P.; Mally, A.; Biemel, K. M.; Lederer, M. O.; Padayatti, P. S. Effect of pyridoxamine on chemical modification of proteins by carbonyls in diabetic rats: characterization of a major product from the reaction of pyridoxamine and methylglyoxal. *Arch. Biochem, Biophys.* **2002**, *402*, 110–119.

(11) Sang, S.; Shao, X.; Bai, N.; Lo, C. Y.; Yang, C. S.; Ho, C. T. Tea polyphenol (−)-epigallocatechin-3-gallate: a new trapping agent of reactive dicarbonyl species. *Chem. Res. Toxicol.* **2007**, *20*, 1862–1870.

(12) Shao, X.; Bai, N.; He, K.; Ho, C. T.; Yang, C. S.; Sang, S. Apple polyphenols, phloretin and phloridzin: new trapping agents of reactive dicarbonyl species. *Chem. Res. Toxicol.* **2008**, *21*, 2042–2050.

(13) Xiao, P. G.; Xing, S. T.; Wang, L. W. Immunological aspects of Chinese medicinal plants as antiageing drugs. *J. Ethnopharmacol.* **1993**, *38*, 167–175.

(14) Ban, S. H.; Kwon, Y. R.; Pandit, S.; Lee, Y. S.; Yi, H. K.; Jeon, J. G. Effects of a bio-assay guided fraction from *Polygonum cuspidatum* root on the viability, acid production and glucosyltranferase of mutans streptococci. *Fitoterapia* **2009**, in press.

(15) Chen, Y.; Wang, M.; Rosen, R. T.; Ho, C. T. 2,2-Diphenyl-1-picrylhydrazyl radical-scavenging active components from *Polygonum multiflorum* Thunb. *J. Agric. Food Chem.* **1999**, *47*, 2226–2228.

(16) Ryu, G.; Ju, J. H.; Park, Y. J.; Ryu, S. Y.; Choi, B. W.; Lee, B. H. The radical scavenging effects of stilbene glucosides from *Polygonum multiflorum*. *Arch. Pharm. Res.* **2002**, *25*, 636–639.

(17) Wang, X.; Zhao, L.; Han, T.; Chen, S.; Wang, J. Protective effects of 2,3,5,4′-tetrahydroxystilbene-2-*O*-β-D-glucoside, an active component of *Polygonum multiflorum* Thunb., on experimental colitis in mice. *Eur. J. Pharmacol.* **2008**, *578*, 339–48.

(18) Lv, L.; Gu, X.; Tang, J.; Ho, C. T. Antioxidant activity of stilbene glycoside from *Polygonum multiflorum* Thunb. in vivo. *Food Chem.* **2007**, *104*, 1678–1681.

(19) Fang, X.; Qiu, F.; Yan, B.; Wang, H.; Mort, A. J.; Stark, R. E. NMR studies of molecular structure in fruit cuticle polyesters. *Phytochemistry* **2001**, *57*, 1035–1042.